Biogeosciences Discuss., https://doi.org/10.5194/bg-2018-448
Manuscript under review for journal Biogeosciences
Discussion started: 19 November 2018

Particulate trace metal dynamics in response to increased CO_2 and iron availability in a coastal mesocosm experiment

M. Rosario Lorenzo[1], María Segovia[1], Jay T. Cullen[2], and María T. Maldonado[3]

[1]Department of Ecology, Faculty of Sciences, University of Málaga, Bulevar Louis Pasteur s/n, 29071-Málaga, Spain
[2]School of Earth and Ocean Sciences, University of Victoria, 3800 Finnerty Road, Bob Wright Centre A405, Victoria BC V8P 5C2
Canada
[3]Department of Earth and Ocean and Atmospheric Sciences, University of British Columbia, 2207 Main Mall, Vancouver BC V6T 1Z4, Canada

Correspondence to: María Segovia (segovia@uma.es) and María T. Maldonado (mmaldonado@eos.ubc.ca)

Abstract. Rising concentrations of atmospheric carbon dioxide are causing ocean acidification and will influence marine processes and trace metal biogeochemistry. The importance of the combined impacts of elevated CO_2 and changes in trace metal availability on marine plankton remain largely unknown. A mesocosm experiment was performed to study changes in particulate trace metal concentrations during a bloom dominated by the coccolithophore *Emiliania huxleyi*. We employed a full-factorial experimental design, comprising all combinations of ambient and elevated pCO_2 and dissolved iron (dFe). Particulate metal concentrations (Fe, Cu, Zn, Co, Mn, Cd, Mo, Ti and Pb) were determined by high-resolution inductively coupled plasma mass spectrometry (HR-ICPMS). We examined biogenic and lithogenic sources of particulate metals, and their evolution during the experiment. Biogenic metal concentrations were estimated from bulk particle measurements by comparing phosphorus (P)-normalised quotas with published ratios, as well as concentrations of particulate trace metals in the presence and absence of an oxalate-EDTA wash. Our results demonstrate that particulate Ti and Fe concentrations were dominated by lithogenic material in the fjord. In contrast, particulate Cu, Co, Mn, Zn, Mo and Cd concentrations correlated with P concentrations and phytoplankton biomass, indicative of their strong biogenic character. Furthermore, ocean acidification changed the relative concentrations of particulate metals; a result mainly driven by the effects of ocean acidification on the growth of different phytoplankton phyla. This study demonstrates the utility and robustness of combining trace metal analyses of particles in a controlled mesocosm experiment with manipulations of CO_2 and Fe concentrations using natural assemblages of marine phytoplankton.

Key words: Global change, iron, CO_2, particulate trace metals, dissolved trace metals, mesocosms, *Emiliania huxleyi,* phytoplankton

1. Introduction

Marine phytoplankton contribute half of the world's total primary productivity, sustaining marine food webs and driving the biogeochemical cycles of carbon and nutrients (Field et al., 1998). Annually, phytoplankton incorporate approximately 45 to 50 billion metric tons of inorganic carbon (Field et al., 1998), removing a quarter of the CO_2 emitted to the atmosphere by anthropogenic activities (Canadell et al., 2007). Yet, the atmospheric CO_2 concentration has increased by 40 % since pre-industrial times as a result of anthropogenic CO_2 emissions, producing rapid changes in the global climate system (Stocker et al., 2013). The dissolution of anthropogenic CO_2 in seawater, causes shifts in

Biogeosciences Discuss., https://doi.org/10.5194/bg-2018-448
Manuscript under review for journal Biogeosciences
Discussion started: 19 November 2018

the carbonate chemical speciation, and leads to ocean acidification (OA). Marine ecosystems are sensitive to changes in pH because pH strongly affects chemical and physiological reactions (Hoffman et al., 2012). Increased CO_2 in seawater may enhance or diminish phytoplankton productivity (Mackey et al., 2015), decrease the $CaCO_3$ production in most planktonic calcifiers (Riebesell and Tortell 2011), and/or inhibit organic nitrogen and phosphorus acquisition (Hutchins et al., 2009). Thus, the biogeochemical cycling of nutrients is predicted to be highly affected by OA (Hutchins et al. 2009). In addition, variations in pH will affect the distribution and speciation of trace metals in the ocean (Millero et al., 2009).

Trace metals, including Fe, Zn, Mn, Cu, Co and Mo, are essential for biological functions (e.g. photosynthesis, respiration and macronutrient assimilation), and Cd can supplement these functions. Thus, trace metals availability can influence phytoplankton growth and community structure (Morel and Price, 2003). In turn, plankton control the distribution, chemical speciation, and cycling of trace metals in the sea (Sunda, 2012), by, for example, releasing organic compounds that dominate the coordination chemistry of metals, internalizing trace elements into the cells, and reducing and/or oxidizing metals at the cell surface. The chemistry of redox speciation of active trace elements is highly dependent on pH. For instance, Fe occurs in two main redox states in the environment: oxidized ferric Fe (Fe (III)), which is poorly soluble at circumneutral pH; and reduced ferrous Fe (Fe (II)), which is easily soluble and therefore more bioavailable. Fe speciation and bio- availability are dynamically controlled by the prevalent changing redox conditions. Also, as the ocean becomes more acidic, reduction of Cu (II) will increase, as the ionic form of Cu (II) is reduced to Cu (I) (Millero et al., 2009). The effect of higher concentrations of Cu(I) in surface waters on biological systems is not well known. Therefore, while the effects of OA on inorganic metal speciation will be more pronounced for metals that form strong complexes with carbonates (e.g. copper) or hydroxides (e.g. iron and aluminium), those that form stable complexes with chlorides (e.g. cadmium) will not be greatly affected. Thus, pH mediated changes in concentrations and/or speciation could possibly enhance trace metal limitation and/or toxicity to marine plankton (Millero et al., 2009).

Iron is crucial for phytoplankton growth because of its involvement in many essential physiological processes, such as photosynthesis, respiration, and nitrate assimilation (Behrenfeld and Milligan, 2013). The decrease in seawater pH in response to OA may increase Fe solubility (Millero et al., 2009), but it may also result in unchanged or lower Fe bioavailability, depending of the nature of the strong organic Fe ligands (Shi et al., 2010). Consequently, changes in iron bioavailability due to ocean acidification can affect positively or negatively ocean productivity and CO_2 drawdown. Copper is an essential micronutrient but may be toxic at high concentrations (Semeniuk et al., 2016). An increase in free cupric ion concentrations in coastal areas due to ocean acidification (Millero et al., 2009) could result in negative effects on phytoplankton. From the open-ocean to coastal areas, the concentration of metals differ, as well as the trace metal requirements of phytoplankton (Sunda and Huntsman, 1995a), and their tolerance to metal toxicity. Accordingly, changes in pH may promote an increase in Cu toxicity in coastal phytoplankton, or enhance Fe limitation in the open ocean. Given that trace metals are essential for phytoplankton productivity, and that are actively internalized during growth, it is important to study the impacts of ocean acidification in the trace metal content of ecologically significant plankton species.

In a rapidly changing global environment, generated by anthropogenic CO_2 emissions, it is critical to gain adequate understanding about ecosystem responses. Due to the complex interactions in aquatic ecosystems such predictions have so far not been possible to do based upon observational data and modelling alone. However, direct empirical studies on natural communities offer a robust tool to analyse interactive effects of multiple stressors. Specifically, mesocosm

Biogeosciences Discuss., https://doi.org/10.5194/bg-2018-448
Manuscript under review for journal Biogeosciences
Discussion started: 19 November 2018

experiments allow perturbation studies with a high degree of realism compared to other experimental systems (Riebesell et al., 2010, Stewart et al., 2013, Riebesell and Gatusso, 2015).

In the present work a bloom of the coccolithophorid *Emiliania huxleyi* was induced in a mesocosm experiment to examine the interactive effects of increased CO_2 and/or dissolved iron on its growth and physiology (Segovia et al., 2017, Segovia et al., 2018, Lorenzo et al., 2018). *Emiliania huxleyi* is the most cosmopolitan and abundant coccolithophore in the modern ocean (Paasche, 2002). Coccolithophores play a key role in the global carbon cycle because they produce photosynthetically organic carbon, as well as particulate inorganic carbon through calcification. These two processes foster the sinking of particulate organic carbon to the deep ocean carbon export (Hutchings, 2011) and impact organic carbon burial in marine sediments (Archer, 1991, Archer and Maier-Reimer., 1994). However, OA will disproportionally affect the abundance of coccolithophores, as well as their rates of calcification and organic carbon fixation (Zondervan et al., 2007). The aim of the present study was to characterize the changes in particulate trace metal concentrations during the bloom of *E. huxleyi* given realistic changes in CO_2 and Fe bioavailability.

2. Materials and methods

2.2 Experimental set-up

The experimental work was carried out in June 2012 in the Raunefjord, off Bergen, Norway as described in detail by Segovia et al., (2017). Twelve mesocosms (11 m^3 each) were set-up in a fully factorial design with all combinations of ambient and elevated pCO_2 and dFe in three independent replicate mesocosms. The mesocosms were covered by lids (both transparent to PAR and UVR) and filled with fjord water from 8 m depth. We achieved two CO_2 levels corresponding to present (390 ppm, LC) and those predicted for 2100 (900 ppm, HC) by adding different quantities of pure CO_2 gas (Shulz et al., 2009). The specific CO_2 concentration and the CO_2 inlet flows in the mesocosms were measured by non-dispersive infrared analysis by using a Li-Cor (LI-820) CO_2 gas analyser (Li-COR, Nebraska, USA) and CO_2 AirSense-310 sensors (Digital Control Systems, Inc, USA). CO_2 concentrations in the mesocosms were calculated from pH and total alkalinity measurements using the CO_2 SYS software (Robbins et al,. 2010). At the beginning of the experiment, nitrate (10 µM) and phosphate (0.3 µM final concentrations) were manipulated to induce a bloom of the coccolithophore *Emiliania huxleyi*. Iron was also manipulated by addition of 70 nM of the siderophore desferrioxamine B (DFB) to half of the mesocosms on day 7, promoting two different iron conditions (+DFB, high dissolved iron; and –DFB, ambient dissolved iron). By day 17, dissolved iron concentrations were ~3-fold higher in the high CO_2 and DFB treatments than the control. The multifactorial experimental design consisted of triplicate mesocosms per treatment and the combinations of high and ambient pCO_2 and dFe levels, resulting in a total of 12 mesocosms: LC-DFB (control), LC+DFB, HC+DFB and HC-DFB. Water samples from each mesocosm were taken from 2 m depth by gentle vacuum pumping of 25 L volume into acid-washed carboys that were quickly transported to the onshore laboratory. The biological and chemical variables analysed were phytoplankton abundance and species composition, dissolved Fe and Cu concentrations (dFe , dCu), nutrient concentrations (nitrate, phosphate, silicic acid and ammonium) and particulate trace metal concentrations.

2.3 Dissolved copper

Low density polyethylene (LDPE) bottles were cleaned with 1% alkaline soap solution for one week, then filled with 6 M trace metal grade HCl and submerged in a 2 M HCl bath for one month. For transport, they were filled with 1 M trace metal grade HCl (Fisher Chemicals) for one more month and kept double bagged. In between each acid treatment, the bottles were rinsed with Milli-Q water (Millipore; hereafter referred to as MQ). Before sampling, the bottles were rinsed three times with filtered seawater. Seawater was collected from each mesocosm, filtered through 0.2 µM

Biogeosciences Discuss., https://doi.org/10.5194/bg-2018-448
Manuscript under review for journal Biogeosciences
Discussion started: 19 November 2018

AcroPak Supor membrane capsule filters into the trace metal clean LDPE bottles, and acidified with ultra-clean HCl (Seastar) in a Class 100 laminar flow hood. Total dissolved Cu concentrations were measured following Zamzow et al., (1998) using a flow injection analysis chemiluminescence detection system (CL-FIA, Waterville Analytical). Total dissolved Fe concentrations were measured as described in Segovia et al., (2017) for this very experiment.

2.4 Particulate metals

2.4.1 Sampling

All equipment used during this study was rigorously acid-washed under trace metal clean conditions. Filters were precleaned with 10% trace metal hydrochloric acid (Fisher, trace metal grade) at 60 °C overnight and were rinsed with Milli-Q (MQ) water. Seawater samples (1-3.5 L) were filtered gently onto 0.45 µm acid washed Supor ®-450 filters on days 12, 17 and 21 of the experiment. Four replicates were taken from each mesocosm. Two filters were analysed without manipulation and the other two were individually washed with oxalate reagent to remove extracellular Fe (Tang and Morel, 2006). Immediately following filtration, the treated filters were soaked in an EDTA–oxalate solution, by adding 20 mL of oxalate solution to the headspace of the Swinnex holders with an acid-washed polypropylene syringe. After 10 min, vacuum was applied to remove the oxalate solution and 10 mL of 0.2 µM filtered chelexed synthetic oceanic water (SOW) solution was passed through the filter to rinse off any remaining oxalate solution. Replicate filters that were not treated with oxalate solution were transferred directly to centrifuge tubes for storage. The filters with particles were frozen in acid-washed 2 mL PP tubes and then, dried and stored until analysis.

2.4.2 Analytical methods

Filters were digested in 7-mL acid-washed Teflon (Teflon, Rochester, NY, USA) vials. Teflon vials were also precleaned using 10% trace metal hydrochloric acid (Fisher, trace metal grade) during two days and then, with nitric acid (Fisher, trace metal grade) at 70 ºC during three days. In between each acid treatment, the bottles were rinsed with MQ. Samples were digested in 3 mL of HNO_3 and 0.5 mL of HF (Fisher, trace metal grade) with lids on for 1 h on a hot plate at 200 ºC. The lids were then removed to evaporate HF at 200ºC. After this, 1.5 mL of HNO_3 were added and the samples were heated with lids on overnight at 150 ºC. Finally, 2.25 mL of $HClO_4$ (Fisher, Optima grade) were added and the samples were heated for 4 h at 200 ºC. After complete digestion, the samples were dried on hot plates at 200ºC. The dried samples were dissolved in 1% nitric acid with 1 ppb in internal standard. The analysis was performed using a high-resolution inductively coupled plasma-mass spectrometer (ICP-MS, Element XR, Thermo Scientific) and the described instrumental settings (Table 1). Filter blanks were collected and subjected to the same storage, digestion, dilution, and analysis processes, and these blank values were subtracted from sample measurements. Particulate samples for ICPMS analysis were processed in a trace metal-clean laboratory under a trace metal-clean laminar flow fume hood.

2.5 Statistical analyses

Data were checked for normality (by Shapiro-Wilks' test), homoscedasticity (by Levene's test) and sphericity (by Mauchly's test). All data met the requirements to perform parametric tests. Statistical significance of treatment effects was carried out using Split-Plot ANOVA followed by post-hoc Sidak and Bonferroni tests (considering $P < 0.05$ as significant). All analyses were performed using the General Linear Model (GLM) procedure. The correlation between variables was analysed by Pearson's product-moment multiple comparisons (considering $P < 0.05$ as significant). Statistical analyses were carried out using SPSS v22 (IBM statistics) and Sigmaplot 12 (Systat Software, Chicago, USA).

Biogeosciences Discuss., https://doi.org/10.5194/bg-2018-448
Manuscript under review for journal Biogeosciences
Discussion started: 19 November 2018

3. Results

3.1 Biological and chemical characteristics during the bloom

All the biological and chemical variables measured during the experiment are presented in Table 2. At the beginning of the experiment (days 1-10, phase 1) a bloom of large chain-forming diatoms was observed, which declined by day 7. This diatom bloom was associated with a sharp decreased in nitrate and silicic acid concentrations. Picoeukaryotes, dominated the phytoplankton community on day 8 (Segovia et al., 2017). During the first 10 days of the experiment, there were no significant differences in the variables measured between the treatments. On day 7, DFB was added to half of the mesocosms (+DFB treatments). An increase in dFe was observed in all treatments between day 7 and 17 (Segovia et al., 2017). This increase in dFe was sustained for the entire experiment in the DFB treatments (Table 2). Dissolved Cu concentrations were not affected by the different treatments (Table 2). After day 10, a bloom of the coccolithophore *Emiliania huxleyi* developed under LC +DFB condition, out-competing the rest of the plankton groups. This bloom was not observed either in the control treatment (LC-DFB) or in the HC treatments, although *E. huxleyi* was still the most abundant species in all treatments; the exception was the HC-DFB treatment (Segovia et al., 2017).

3.2 Particulate metal concentrations changed during the Emiliania huxleyi bloom

The particulate trace-metal concentrations (nmol L^{-1}, mean of all treatments and dates) during the development of the bloom of *E. huxleyi* were highest for Al, Fe and Zn, and lowest for Cd, following this trend: Al ≈ Fe ≈ Zn > Ti > Cu ≈ Mn > Mo ≈ Pb > Co > Cd. Significant changes in trace metals concentrations were observed for Fe, Cu, Co, Zn, Cd, Mn, Mo and Pb over time, while Ti and Al were unaffected (Table 3 and Table 5). The only metal that showed a time-dependent decrease in its particulate concentration was Fe (Table 3, except for LC-DFB, day 17). In general, the treatments with the highest particulate metals concentrations also exhibited the highest particulate P, except for Al, Ti, Fe, and Pb (Table 3). On days 12 and 17, the highest particulate metals concentrations were observed in the LC+DFB, while on day 21, they were observed in both LC treatments (Table 3).

3.3 Increased CO_2 and the DFB addition affected particulate metal concentrations

Increased CO_2 and DFB additions did not affect the concentrations of particulate Al, Cu, Ti and Pb. However, while the addition of DFB did not directly influence particulate concentrations of Fe and Cd, high CO_2 had a negative impact on particulate Fe. Particulate Cd concentrations were also inversely affected by CO_2, but mainly in the presence of DFB (CO_2; and CO_2 x DFB effect, Table 5). All other elements (P, Co, Zn, Mn and Mo) exhibited significant effects by CO_2 and DFB, and the interaction between these two factors was clear (Table 5). For example, Zn concentrations were highest in the LC treatment, but only with the addition of DFB.

3.4 Except for Al and Ti, oxalate-wash reduced all particulate metal concentrations

To better estimate the biogenic fraction of the particulate metals, the filters were washed with an oxalate-EDTA solution, which removes extracellular metals and oxyhydroxides (Tang and Morel., 2006). The only two elements unaffected by the oxalate wash were Al and Ti. All other elements showed significantly lower concentrations in the oxalate-treated than in untreated samples (Table 3 vs. 4). The quantity of metal remaining after the oxalate wash (ie. biogenic fraction) varied among elements. Biogenic concentrations of the most labile elements—Pb, Mo, Cd, Zn, Cu and Mn—comprised 30–60% of total particulate metals, while 70–80% of total particulate Co, Fe, and P remained in the biogenic fraction (Table 4). As a general trend, the elements showed the highest concentrations in the LC+DFB treatment at the beginning of the bloom (day 12) after the oxalate wash. At the end of the experiment, the highest trace element concentrations were obtained in the LC treatments, with the exception of Pb (Table 4).

Biogeosciences Discuss., https://doi.org/10.5194/bg-2018-448
Manuscript under review for journal Biogeosciences
Discussion started: 19 November 2018

3.5 After oxalate-wash P, Fe, Co, Zn Mn and Mo were less affected by increased CO_2 and the DFB addition

The effects of CO_2 and DFB on particulate metal concentrations were different for the oxalate-treated and untreated samples. All the elements, except Mn and Cu, showed significant differences over time (Table 5). Cobalt concentrations were negatively affected by high CO_2 levels. In contrast, DFB only induced changes in the particulate concentrations of Zn and Ti. Zinc concentrations showed a strong interaction between CO_2 and DFB, and the highest concentrations of this metal occurred in the LC+DFB treatment.

3.6 Fe and Ti were associated with lithogenic sources

The Fe:P and Ti:P ratios were relatively similar to crustal ratios. In addition, significant positive correlations were observed between Me:P and Al:P for Fe and Ti (Figure 5). These results suggest that particulate Fe and Ti were determined by lithogenic inputs. Iron:P and Ti:P were not significantly affected by increased CO_2 and/or DFB addition, but showed significant differences over time (Table 7). Samples washed with oxalate-EDTA solution showed significant differences in Fe concentrations due to DFB addition. There was no significant relationship between particulate Fe and Ti concentrations (with or without oxalate wash) with either the total plankton (phytoplankton and microzooplankton) or *E. huxleyi* biomass (Table 6).

3.7 Co, Cu, Zn, Cd, Mn and Mo were associated with phytoplankton

The comparison of the P-normalized quotas with Al:P showed no correlations with Co, Cu, Zn, Cd, Mn and Mo (Figure 1), indicating that these particulate metals were non-lithogenic. Compared to the ratios of trace metal to phosphorous (Me:P) in marine plankton assemblages (Ho, 2006) our measured ratios were similar for Cu, higher for Mn and Zn, and lower for Co and Cd (Figure 1). Furthermore, the metal ratios we measured (Me:P) were higher for Cu, Zn and Mo, and lower for Mn, Co and Cd, than the ratios published for *E. huxleyi* (Figure 1). Copper, Co and Zn:P ratios changed significantly over time (Table 7). Copper, Co, Zn and Mn:P ratios showed significant effects due to increased CO_2 (Table 7). DFB did not affect Me:P ratios of these elements. In contrast, the oxalate-EDTA washed metal ratios (Me:P) for Cu and Co were significantly influenced by DFB (Table 7). The oxalate washed samples also presented a significant effect of CO_2 on the Cu:P, Co:P, and Zn:P ratios. An interaction between the effects of CO_2 and DFB was detected in Cd:P and Mn:P ratios (Table 7). The concentrations of these metals also showed significant correlations with the biomass of *E. huxleyi* and that of total plankton cells ($p < 0.05$), in both untreated or treated oxalate-washed samples (Table 6).

4. Discussion

We investigated changes in particulate trace metal concentrations, both biogenic and lithogenic, in response to increased CO_2 and Fe availability in a coastal mesocosm experiment dominated by a bloom of the coccolithophore *Emiliania huxleyi*. To combine trace metal analyses of particles in a controlled mesocosm experiment with manipulations of CO_2 and Fe levels using natural assemblages of marine phytoplankton is a powerful approach that allows us to address key questions. Our results demonstrate that in the studied fjord, particulate Ti and Fe concentrations were dominated by lithogenic material. In contrast, particulate Cu, Co, Mn, Zn, Mo and Cd concentrations were correlated with P concentrations, as well as phytoplankton biomass, suggesting strong biogenic influence on their distribution (Table 6). The concentrations of these biogenic metals in the *E. huxleyi* bloom were ranked as: Zn > Cu ≈ Mn > Mo > Co > Cd. Changes in CO_2 and/or Fe levels affected total particulate and biogenic metal concentrations for some metals. Changes in CO_2 had the most significant effect on particulate Fe concentrations. In contrast, the effects of CO_2 on the Me:P ratios were only detected in Co, Cu, Zn, and Mn.

Biogeosciences Discuss., https://doi.org/10.5194/bg-2018-448
Manuscript under review for journal Biogeosciences
Discussion started: 19 November 2018

4.1 Efficacy of the oxalate-EDTA wash removing lithogenic trace metals from particles

The oxalate–EDTA reagent was developed to remove surface-adsorbed Fe prior to particulate trace metal analyses (Tovar-Sanchez et al., 2003). This reagent works primarily through ligand-promoted dissolution via complexation both to EDTA and oxalate (Tovar-Sanchez et al., 2003, Tang and Morel, 2006). In this study, the oxalate wash significantly decreased the concentration of all particulate metals, with the exception of Al and Ti (Table 4), as observed by Rauschenberg and Twining (2015). In general, the concentrations of Fe and Co in the particles were decreased the least by the oxalate wash (by ~ 25%), while Mo and Pb concentrations were decreased the most (by ~70%). The concentrations of particulate Cu, Zn, Cd and Mn were reduced by 50% by the oxalate wash. As shown previously (Sanudo-Wilhelmy et al. 2004), the oxalate reagent also removed extracellular P (by ~20%). Compared to Rauschenberg and Twining (2015), the estimates of the biogenic fraction, after the oxalate wash, were in agreement for Co, Cu and P, and lower for Fe, Mn, Zn and Cd concentrations. The efficacy of the oxalate wash to dissolve Fe, and other metals, from lithogenic particles is not well constrained (Frew et al. 2006, Rauschenberg and Twining, 2015, King et al., 2012). Therefore, the results obtained after the oxalate-EDTA wash should be interpreted with caution because we do not know whether the removed metal fraction is a) only lithogenic; b) mainly lithogenic but some biogenic fraction is also removed, or c) whether metals absorbed onto particles are equally labile to the wash on biogenic and lithogenic particles. However, some of the trends we observed [eg. higher Me concentrations in the LC+DFB treatments (Table 4); or positive correlations between phytoplankton biomass and Me concentrations (Table 6)] were identical for the oxalate-EDTA washed and non-washed particles. Thus, below we focus our discussion on the non-oxalate wash results.

4.2 Particulate elements (P, Cu, Co, Zn, Cd, Mn and Mo) were mainly associated with phytoplankton

Certain particulate elements (P, Cu, Co, Zn, Cd, Mn and Mo) were clearly biogenic. Three lines of evidence are presented in support of this. First, the total biomass of phytoplankton exhibited a significant positive correlation with particulate P (Table 6), suggesting that most particulate P was biogenic, as shown previously (Ho et al., 2007, Ho et al., 2009). The concentrations of Cu, Co, Zn, Cd, Mn and Mo also exhibited positive significant correlations with the biomass of total cells (phytoplankton and microzooplankton) or *E. huxleyi* (Table 6), indicating that these particulate metals were also associated with phytoplankton. Second, the Me:P ratios are not similar to crustal ratios. Third, the Me:P ratios we measured in the particles are similar to those of natural phytoplankton assemblages (Ho, 2006) and of *Emiliania huxleyi* cultures (Ho et al., 2003).

The concentrations of biogenic metals in the studied *Emiliania huxleyi* bloom were ranked as: Zn > Cu ≈ Mn > Mo > Co > Cd (Table 3), similar to those reported in indigenous phytoplankton populations: Fe ≈ Zn > Mn ≈ Ni ≈ Cu ≫ Co ≈ Cd, (Twining and Baines, 2013). Particulate Zn concentrations were especially high in the LC+DFB treatment, where the highest *E. huxleyi* biomass was observed. The only treatment where E. *huxleyi* did not dominate the community was the HC-DFB. In this treatment, the particulate trace metal ranking was the same, but their concentrations were higher than those in HC+DFB on day 17. At the end of the experiment, the metal concentrations in both HC treatments were comparable and, similar effect of both factors (increased CO_2 and the addition of DFB) were observed (lower values in HC treatments, Table 3).

Emiliania huxleyi is well known for its high Zn cellular requirements (Sunda, 2012). This trace metal serves as a cofactor in enzymes involved in biochemical processes, such as alkaline phosphatase, RNA polymerase, or superoxide dismutase (Cu/Zn-SOD). An increase in dissolved Zn levels can stimulate the growth of *E. huxleyi* in natural communities but its effect is less pronounced than that of dissolved Fe (Crawford et al., 2003). The cellular

Biogeosciences Discuss., https://doi.org/10.5194/bg-2018-448
Manuscript under review for journal Biogeosciences
Discussion started: 19 November 2018

concentrations of Zn, Co and Cd in marine microalgae are highly interdependent (Price and Morel, 1990; Sunda and Huntsman, 1995b; Jakuba et al,. 2008) because these metals have similar size/charge ratios (Zn and Co) or chemical nature (Zn and Cd) and thus can substitute for each other in certain biochemical functions, as it has been demonstrated for *E. huxleyi* (Xu et al., 2007). However, if available, *E. huxleyi* has a preference for Zn (Sunda and Huntsman, 1995b). Our results support these findings, showing significantly higher particulate concentrations of Zn, and Zn:P ratios than those of Co and Cd (Table 3, Figure 1).

Though, it is well known that *E. huxleyi* has higher Zn requirements relative to those of other phytoplankton, the unique physiological functions of Zn in *E. huxleyi* are still unresolved. Indeed, we currently know very little about the molecular mechanisms of Zn acquisition and homeostasis in eukaryotic phytoplankton, and in coccolithophores in particular. However, the presence of genes encoding for Zn-metalloproteins in the *Emiliania huxleyi* genome (Read et al., 2013) provide further evidence for the importance of Zn nutrition in this coccolithophore. For example, we have found alpha, beta and gamma carbonic anhydrases annotated genes encoding for enzymes involved in carbon concentrating mechanisms (CCMs). Interestingly, we also found a putative ZIP-transporter gene. ZIP-transporters are involved in Zn uptake, and are able to regulate Zn transport under high Zn to prevent intracellular Zn toxicity. Genes encoding for Zn fingers proteins are also present in the genome. The functions of these proteins are extremely diverse and include DNA recognition, RNA packaging, transcriptional activation, regulation of apoptosis, etc. We also found a putative DNAJ gene (also known as Hsp40 or DNAJ heat-shock proteins encoding gene). These heat-shock proteins protect other proteins from irreversible aggregation during synthesis or stress conditions. Genes encoding for an RNA polymerase needed for nucleic acid replication and transcription), alkaline phosphatase (involved in the assimilation of P from organic P compounds), and Cu-Zn superoxide dismutase (Cu/Zn-SOD, involved in detoxification of reactive oxygen species) were also found in the genome. However, we did not find in the *E. huxleyi* genome other key common Zn-metalloproteins, such as tRNA synthetase, reverse transcriptase, metallo-carboxypeptidase, ABC-Zn-transporter and CDF-Zn-transporter. *Emiliania huxleyi* plays a major role in the global carbon cycle by regulating the exchange of CO_2 across the ocean-atmosphere interface through photosynthesis and calcium carbonate precipitation (Dymond and Lyle, 1985). Thus, dissolved Zn could indirectly affect the global C pump by influencing the growth of coccolithophores. The ratios (Me:P) obtained for Cu, Co, Cd and Mn in this study were similar to those obtained in studies in the North Atlantic (Tovar-Sanchez, 2006, Nuester et al., 2012). The Co:P and Mn:P were also comparable to published phytoplankton ratios (Figure 1). The dissolved and particulate Cu concentrations in our experiment were high, and similar to those previously measured in this fjord (Muller et al., 2005).

The Cu:P ratios were mainly biogenic, but the values were relatively elevated compared to those of other phytoplankton (Ho et al., 2003, Ho, 2006). Rain events in this fjord result in high dissolved Cu and the active production of strong organic ligands by *Synechococcus*—to lower the free Cu concentrations (Muller et al., 2005). Therefore, high Cu might be a general condition in this fjord, and indigenous plankton might have developed physiological mechanisms to deal with high Cu, such as the production of organic ligands to prevent uptake (Vraspir and Butler, 2009), or of heavy-metal-binding peptides (phytochelatins) to lower Cu toxicity inside the cell (Ahner and Morel, 1995; Ahner et al., 1995; Knauer et al., 1998). Given that we measured high particulate Cu in our experiment but comparable to previous studies (Muller et al., 2005), *E. huxleyi* might have been relying mainly on phytochelatins to buffer high intracellular Cu or on other detoxification mechanisms (Ahner et al., 2002). Indeed, in the genome of *E.huxleyi*, we found a gene encoding for a hypothetical protein with high homology to a phytochelatin synthase, required for tolerating metal toxicity. Alternatively, Cu might be particularly important for the growth of this coccolithophore, as indicated by a study with a coastal strain, which had high Cu requirements to maintain maximum growth rate regardless of Fe levels in the media

Biogeosciences Discuss., https://doi.org/10.5194/bg-2018-448
Manuscript under review for journal Biogeosciences
Discussion started: 19 November 2018

(Guo et al., 2012). Therefore, the high concentrations of particulate Cu in the *E. huxleyi* bloom might be due to high dissolved Cu concentration in the fjord, unregulated uptake and/or high Cu requirements.

The Cd:P were significantly lower than those found in phytoplankton and *E. huxley*i. This was surprising, because Cd quotas are normally higher in coccolithophores than in diatoms and chlorophytes (Sunda and Huntsman, 2000; Ho et al., 2003). High Cd quotas in coccolithophores have been suggested to result from accidental uptake through Ca transporters and channels (Ho et al., 2009). The low Cd quotas here may be explained by the antagonistic interaction between Mn and Cd or Zn and Cd under high Mn and Zn, respectively (Sunda and Huntsman, 1998, 2000; Cullen and Sherrell, 2005). The high Zn:P ratios in this study indicate high bioavailability of Zn. Our Mn:P ratios were below those in cultures of *E. huxleyi* (Ho et al. 2003), but in Ho et al (2003) phytoplankton were grown in the presence of high Mn concentrations (Ho et al., 2003), thus the Mn:P ratios reported were suspected to represent luxury Mn uptake. In addition, differences between the Me:P ratios in this experiment and those in previous studies could simply imply different growth conditions (e.g. light levels, macronutrient concentrations, etc.) and the dominance of a few algal species, such as *Emiliania huxleyi* (Ho et al., 2006).

4.3 Fe in bulk particles was mainly lithogenic

Iron enrichment is common in coastal waters, due to sediment resuspension, rivers input, aeolian deposition and mixing or upwelling of deep water. The metal with the highest particulate concentrations in our study was Fe (Table 3). Furthermore, particulate Fe and Ti were the only metals with positive correlations with Al and without correlation with phytoplankton biomass (Figure 1, Table 5), indicating a strong lithogenic component. The similarity between our values Fe:P values and that of the crustal ratio (Figure 1) also supports this finding. Indeed, the Fe:P ratios were significantly higher than those of indigenous plankton assemblages and phytoplankton cultures (Figure 1). We believe that the lithogenic fraction of Fe in the bulk particles in our experiment masked the biogenic signal, as proposed by King et al. (2012). Interestingly, the particulate Fe concentration (nmol L^{-1}) decreased between days 12 and 21 (Table 3 and 5); this could be due to the solubilisation of particulate Fe to the dissolved phase (Kuma et al., 1996, Millero et al., 2009), as demonstrated by the increase in dissolved Fe in treatments with high CO_2 and/or the addition of DFB (Table 1). The sinking of pFe could have resulted in less pFe, as indicated by the lowering of the ratio between the concentration of Fe in particles and that in the dissolved phase (i.e. partition coefficient, Supplemental Figure S2). The decrease in particulate iron concomitant to the increase in dissolved iron up to a significant 12-fold change from particulate iron to dissolved iron in the LC+DFB treatment indicated that DFB mediated the transfer of Fe from the particulate to the soluble pool (Segovia et al., 2017). In addition, high CO_2 also increased dissolved Fe levels (Segovia et al., 2017). Thus, both DFB addition and HC promoted high dFe concentrations in our experiment.

4.4 Effects of high CO_2 and dissolved Fe levels on particulate metal concentrations and Me: P ratios

The concentrations of particulate Al, Ti, Pb and Cu, were unaffected by changes in CO_2 and/or iron levels. However, high CO_2 clearly decreased the concentration of particulate Fe (and increased dissolved Fe) as predicted by Millero et al. (2009). The decrease in particulate Fe might have been due to enhanced solubility of Fe- oxides at low pH. Finally, the concentration of the elements P, Co, Zn, Mn and Mo were influenced by CO_2 and Fe levels, but the interaction between these factors was complex. In general, the highest Me ratios for P, Co, Zn, Mn and Mo were observed in the LC+DFB treatment, where the addition of DFB resulted in higher dissolved Fe, and optimal pH enhanced *E. huxleyi* growth. This promoted metal accumulation in biogenic particles. Elevated CO_2 levels in the mesocosms had a significant effect on the Me:P ratios of Cu, Co, Zn, and Mn. For example, while Zn:P and Mn:P ratios were higher

Biogeosciences Discuss., https://doi.org/10.5194/bg-2018-448
Manuscript under review for journal Biogeosciences
Discussion started: 19 November 2018

under low CO_2, those of Co:P were higher under high CO_2. Thus, the CO_2 effects did not follow a clear trend and were sometimes positive and other times negative.

5. Concluding remarks

Knowledge of the trace metal composition of in situ marine phytoplankton may allow us to estimate how microalgae in the future will influence the relative distribution and vertical transport of trace metals in the ocean. The results presented here showed that except for Ti and Fe, the trace metal concentrations of marine particles during a bloom of *Emiliania huxleyi* were a) highly dynamic, b) positively correlated with plankton biomass, c) influenced by growth requirements, and d) strongly affected by changes in CO_2 and dissolved Fe. According to our results, ocean acidification will decrease *E. huxleyi* abundance, and as a result, the concentration of some particulate trace metals that are especially high in *E. huxleyi,* such as Zn. Most importantly, OA is expected to change the relative concentrations of particulate metals, due to the differential effects of OA on the growth of marine phytoplankton species, and the contrasting metal requirements of phytoplankton phyla. OA might also affect the sinking flux of particulate Fe which would have an impact on the sinking of particulate metals associated with terrestrial material/dust in open ocean settings. Therefore, as suggested by Twining and Baines (2013), we require the development of ecophysiological models that link trace element composition of phytoplankton to physiological performance, as well as ecological models that are able to predict plankton physiological strategies and metal composition in a changing ocean, and the resulting effects of phytoplankton on the biogeochemical cycles of metals under a rapidly changing ocean.

Acknowledgments

This work was funded by CTM/MAR 2010-17216 (PHYTOSTRESS) research grant from the Spanish Ministry for Science and Innovation (Spain) to MS, and by NSERC grants (Canada) to MTM and JTC. MRL was funded by a FPU grant from the Ministry for Education (Spain) and by fellowships associated to the mentioned above research grants to carry out a short-stay at MTM and JTC laboratories to analyse dissolved and particulate metals. We thank all the participants of the PHYTOSTRESS experiment for their collaboration, and the MBS (Espegrend, Norway) staff for logistic support during the experiment.

References

Ahner, B.A., Liping, W., Oleson, J.R., Ogura, N.: Glutathione and other low molecular weight tiols in marine phytoplankton under metal stress, Mar. Ecol. Prog. Ser., 232, 93-103, 2002.

Behrenfeld, M.J., Milligan, A.J.: Photophysiological expressions of iron stress in phytoplankton, Ann. Rev. Mar. Sci. 5, 217–246, 2013.

Canadell, J.G., Quéré, C., Raupach, M.R., Field, C.B., Buitenhuis, E.T., Ciais, P., Conway, T.J., Gillet, N.P., Houghton, R.A., Marland, G.: Contributions to accelerating atmospheric CO_2 growth from economic activity, carbon intensity, and efficiency of natural sinks. Proc. Natl. Acad. Sci. USA 104, 18886-18870, 2007

Crawford, D.W., Lipsen, M.S., Purdie, D.A., Lohan, M.C., Statham, P.J., Whitney, F.A., Putland, J.N., Johnson, W.K., Sutherland, N., Peterson, T.D., Harrison, P.J., Wong, C.S.: Influence of zinc and iron enrichments on phytoplankton growth in the northeastern subarctic Pacific. Limnol. Oceanogr, 48,1583–1600, 2003.

Cullen, J.T., Sherrell, R.M.: Effects of dissolved carbon dioxide, zinc, and manganese on the cadmium to phosphorus ratio in natural phytoplankton assemblages, Limnol. Oceanogr. 50, 1193–1204, 2005.

Dymond, J., Lyle, M.: Flux comparisons between sediments and sediment traps in the eastern tropical Pacific: implications for atmospheric CO_2 variations during the Pleistocene. Limnol. Oceanogr, 30, 699–712, 1985

Field, C.B.: Primary production of the biosphere: Integrating terrestrial and oceanic components, Science 281, 237–240,

1998.

Frew, R.D., Hutchins, D.A., Nodder, S., Sanudo-Wilhelmy, S., Tovar-Sanchez, A., Leblanc, K., Hare, C.E., Boyd, P.W.: Particulate iron dynamics during Fe Cycle in subantarctic waters southeast of New Zealand, Glob. Biogeochem. Cycles 20, GB1S93. http://dx. doi.org/10.1029/2005GB002558, 2006.

Guo, J., Lapi, S., Ruth, T.J., Maldonado, M.T.: The effects of iron and copper availability on the copper stoichiometry of marine phytoplankton. J. Phycol, 48, 312–325, 2012.

Ho, T-Y.: The trace metal composition of marine microalgae in cultures and natural assemblages. In: Rao S (ed) Algal cultures, analogues of blooms and applications, Science Publishers, New Hampshire, p 271–299, 2006.

Ho, T., Quigg, A., Zoe, V., Milligan, A.J., Falkowski, P.G., Morel, M,M.: The elemental composition of some marine phytoplankton. J. Appl. Phycol 1159,1145–1159, 2003

Ho, T-Y., Wen, L-S., You, C-F., Lee, D-C.: The trace metal composition of size-fractionated plankton in the South China Sea: Biotic versus abiotic sources. Limnol. Oceanogr, 52, 1776–1788, 2007.

Ho, T-Y., You, C.F., Chou, W-C., Pai, S-C., Wen, L-S., Sheu, D.D.: Cadmium and phosphorus cycling in the water column of the South China Sea: The roles of biotic and abiotic particles, Mar. Chem. 115-125-133, 2009.

Hoffmann, L.J., Breitbarth, E., Boyd P.W., Hunter, K.A.: Influence of ocean warming and acidification on trace metal biogeochemistry, Mar Ecol Prog Ser 470-191–205, 2012.

Hutchins, D., Mulholland, M., Fu, F.: Nutrient cycles and marine microbes in a CO_2-enriched ocean, Oceanography 22-128–145, 2009.

Jakuba, R.W., Moffett, J.W., Dyhrman, S.T.: Evidence for the linked biogeochemical cycling of zinc, cobalt, and phosphorus in the western North Atlantic Ocean, Global Biogeochem. Cycles 22, GB4012, 2008.

King, A.L., Sanudo-Wilhelmy, S.A., Boyd, P.W., Twining, B.S., Wilhelm, S.W., Breene, C., Ellwood, M.J. and Hutchins, D.A.: A comparison of biogenic iron quotas during a diatom spring bloom using multiple approaches, Biogeosciences 9, 667–687, 2012.

Mackey, K.R.M., Morris, J.J., Morel, F.M.M.: Response of photosynthesis to ocean acidification, Oceanography 28,74–91, 2015.

Millero, F.J., Woosley, R., Ditrolio, B., Waters, J.: Effect of ocean acidification on the speciation of metals in seawater, Oceanography 22:72–85, 2009.

Morel, F.M., Price, N.M.: The biogeochemical cycles of trace metals in the oceans, Science 300, 944–947, 2003.

Muller, F.L., Larsen, A., Stedmon, C.A., Søndergaard, M.: Interactions between algal – bacterial populations and trace metals in fjord surface waters during a nutrient-stimulated summer bloom, Limnol Oceanogr 50, 1855–1871, 2005.

Nuester, J., Vogt, S., Newville, M., Kustka, A.B., Twining, B.S.: The unique biogeochemical signature of the marine diazotroph *Trichodesmium*, Front Microbiol Chem 3,150, 2012.

Paasche, E.: A review of the coccolithophorid *Emiliania huxleyi* (Pymnesiophyceae), with particular reference to growth, coccolith formation, and calcification-photosynthesis interactions, Phycologia 40, 503–529, 2002.

Price, N.M., Morel, F.M.M.: Cadmium and cobalt substitution for zinc in a marine diatom, Nature 344, 658–660, 1990.

Rauschenberg, S., Twining, B.S.: Evaluation of approaches to estimate biogenic particulate trace metals in the ocean, Mar Chem 171, 67-77, 2015

Riebesell, U., Tortell, P.D.: Effects of ocean acidification on pelagic organisms and ecosystems, In: Gatusso J-P, Lansson L (eds) Ocean Acidification. Oxford University Press., Oxford, p 99–121, 2011.

Robbins, L.L., Hansen, M.E., Kleypas, J.A., Meylan, S.C.: CO_2calc: A User Friendly Carbon Calculator foe Windows, Mac OS X and iOS (iPhone), Open File Rep. 2010-1280, 2010.

Sanudo-Wilhelmy, S.A., Tovar-Sanchez, A., Fu, F.X., Capone, D.G., Carpenter, E.J., Hutchins, D.A.: The impact of surface-adsorbed phosphorus on phytoplankton Redfield stoichiometry, Nature 432, 897–901, 2004.

469 Semeniuk, D.M, Bundy, R.M., Posacka, A.M., Robert, M., Barbeau K.A., Maldonado, M.T.: Using ^{67}Cu to study the
470 biogeochemical cycling of copper in the northeast subarctic Pacific ocean, Frontiers Mar. Sci. 3, 2-19, 2016.
471 Segovia, M., Lorenzo, M.R., Maldonado, M.T., Larsen, A., Berger, S.A., Tsagaraki, T.M., Lázaro, F.J., Iñiguez, C.,
472 García- Gómez, C., Palma, A., Mausz, M.A., Gordillo, F.J.L., Fernández, J.A., Ray, J. L., Egge, J.K.: Iron availability
473 modulates the effects of future CO_2 levels within the marine planktonic food web, Mar. Ecol. Progr. Ser. 565, 17–33,
474 2017.
475 Shi, D., Xu, Y., Hopkinson, B.M., Morel, F.M.M.: Effect of ocean acidification on iron availability to marine
476 phytoplankton, Science 327, 676–679, 2010.
477 Stocker, T.F., Qin, D., Plattner, G-K., Tignor, M., Allen, S.K., Boschung, J., Nauels, A., Xia, Y., Bex, V., Midgley,
478 P.M. (Eds) IPCC, 2013: Climate Change 2013: The Physical Science Basis. Contribution of Working Group I to the
479 Fifth Assessment Report of the Intergovern- mental Panel on Climate Change. Cambridge University Press,
480 Cambridge, United Kingdom and New York, NY, USA, 2013.
481 Sunda, W.G., Huntsman, S.A.: Iron uptake and growth limitation in oceanic and coastal phytoplankton, Mar. Chem. 50,
482 189–206, 1995a.
483 Sunda, W.G., Huntsman, S.A.: Cobalt and zinc interreplacement in marine phytoplankton: biological and geochemical
484 implications, Limnol. Oceanogr. 40, 1404–1417, 1995b.
485 Sunda, W.G., Huntsman, S.A. Control of Cd concentrations in a coastal diatom by interactions among free ionic Cd,
486 Zn, and Mn in seawater, Environ Sci Technol 32:2961–2968, 1998.
487 Sunda, W.G., Huntsman, S.A.: Effect of Zn, Mn, and Fe on Cd accumulation in phytoplankton: implications for oceanic
488 Cd cycling, Limnol. Oceanogr. 45, 1501–1516, 2000.
489 Sunda, W.G.: Feedback interactions between trace metal nutrients and phytoplankton in the ocean, Front Microbiol 3,
490 204, 2012.
491 Tang, D.G.,Morel, F.M.M.: Distinguishing between cellular and Fe-oxide-associated trace elements in phytoplankton,
492 Mar. Chem. 98, 18–30, 2006.
493 Taylor, S.: Abundance of chemical elements in the continental crust: a new table. Geochim Cosmochim Acta 28, 1273–
494 1285, 1964.
495 Tovar-Sanchez, A., Sanudo-Wilhelmy, S.A., Garcia-Vargas, M., Weaver, R.S., Popels, L.C., Hutchins, D.A.: A trace
496 metal clean reagent to remove surface-bound iron from marine phytoplankton, Mar. Chem. 82, 91–99, 2003.
497 Tovar-Sanchez, A., Sanudo-Wilhelmy, S.A., Kustka, A.B., Agustí, S., Dachs, J., Hutchins, D.A., Capone, D.G. and
498 Duarte, C.M.: Effects of dust deposition and river discharges on trace metal composition of Trichodesmium spp. in
499 the tropical and subtropical North Atlantic Ocean, Limnol Oceanogr 51, 1755–61, 2006.
500 Twining, B.S., Baines, S.B.: The trace metal composition of marine phytoplankton, Ann Rev Mar Sci 5, 191–215,
501 2013.
502 Xu, Y., Tang, D., Shaked, Y., Morel, F.M.M.: Zinc, cadmium, and cobalt interreplacement and relative use efficiencies
503 in the coccolithophore *Emiliania huxleyi*, Limnol Oceanogr 52, 2294–2305, 2007.
504 Zamzow, H., Coale, K.H., Johnson, K.S.,Sakamoto, C.M.: Determination of copper complexation in seawater using
505 flow injection analysis with chemiluminescence detection, Anal Chim Acta 377, 133–144, 1998.
506 Zondervan, I.: The effects of light, macronutrients, trace metals and CO_2 on the production of calcium carbonate and
507 organic carbon in coccolithophores–A review, Deep Sea Res Part II Top Stud Oceanogr 54,521–537, 2007.

Biogeosciences Discuss., https://doi.org/10.5194/bg-2018-448
Manuscript under review for journal Biogeosciences
Discussion started: 19 November 2018

508 **Table 1.** Instrumental conditions of ICP-MS and measurement parameters used during determination of trace elements concentrations.

Instrument conditions	
Instrument type	ELEMENT XR
Torch	Fassel type
Spray chamber	Glass cyclonic spray chamber
Nebuliser	ESI microflow ST nebuliser (self aspirating)
Cones	Standard Ni sampler and skimmer
RF Power (W)	1120
Cooling gas flow rate (L min^{-1})	16
Auxiliary gas flow rate (L min^{-1})	0.9
Sample gas flow rate (L min^{-1})	1.2
Sample matrix	1% nitric acid
Method acquisition parameters	
Scan type	E-scan
Spectral resolution	Low (nominal m/Δm~300)
Isotopes of interes	Medium (nominal m/Δm~3000) ^{95}Mo ^{98}Mo ^{111}Cd ^{114}Cd ^{206}Pb ^{208}Pb ^{27}Al ^{31}P ^{47}Ti ^{49}Ti ^{55}Mn ^{56}Fe ^{59}Co ^{63}Cu ^{65}Cu ^{66}Zn ^{68}Zn
Internal standard	^{115}In
Mass window (%)	40
Samples/peak	10
Samples time (ms)	10
Runs	3
Passes	10

509

510

Biogeosciences Discuss., https://doi.org/10.5194/bg-2018-448
Manuscript under review for journal Biogeosciences
Discussion started: 19 November 2018

Table 2. Biological and chemical characteristics of the different treatments; LC: ambient CO_2 (390 µatm); HC: increased CO_2 (900 µatm); -DFB (ambient dFe); +DFB (increased dFe) during the development of a bloom of *Emiliania huxleyi*. All the data except dCu concentration were obtained from Segovia et al. 2017. Data are averages of replicate mesocosms and standard deviations are shown in brackets.

Treatment	CO_2 (µatm)	dFe (nM)	dCu (nM)	Nitrate (µM)	Phosphate (µM)	Silicate (µM)	Ammonium (µM)	Dominant size group	*E. huxleyi* abundance (cell/mL)
Before Emiliania huxleyi bloom (d6)									
LC-DFB	376 (9)	4.62 (0.33)	7.83 (0.83)	2.15 (0.48)	0.05 (0.03)	0.80 (0.20)	0.14 (0.07)	Picoeukaryotes	~1500
LC+DFB	388 (27)	4.45 (0.46)	7.75 (0.29)	2.16 (0.17)	0.05 (0.05)	0.78 (0.22)	0.06 (0.07)	Picoeukaryotes	~1500
HC+DFB	888 (38)	5.46 (0.98)	7.47 (0.45)	1.97 (0.54)	0.04 (0.03)	0.90 (0.08)	0.11 (0.04)	Picoeukaryotes	~1500
HC-DFB	930 (68)	5.27 (0.02)	7.30 (0.22)	2.47 (0.08)	0.04 (0.04)	0.71 (0.31)	0.08 (0.03)	Picoeukaryotes	~1500
d12									
LC-DFB	231 (27)	5.56 (1.85)	8.68 (0.45)	0.03 (0.06)	0.07 (0.06)	0.31 (0.03)	0.80 (0.19)	*Emiliania huxleyi*	~2000
LC+DFB	278 (33)	6.59 (0.29)	7.83 (0.31)	0.05 (0.04)	0.03 (0.03)	0.49 (0.07)	1.24 (0.13)	*Emiliania huxleyi*	~10000
HC+DFB	1112 (64)	8.66 (1.19)	7.44 (0.53)	0.02 (0.03)	0.03 (0.01)	0.40 (0.04)	0.61 (0.15)	*Emiliania huxleyi*	~5000
HC-DFB	1056 (21)	7.46 (0.57)	8.39 (0.23)	0.04 (0.04)	0.02 (0.01)	0.32 (0.03)	0.79 (0.14)	*Emiliania huxleyi*	~5000
d17									
LC-DFB	245 (31)	3.66 (0.52)	7.54 (0.79)	0.12 (0.11)	0.08 (0.04)	0.37 (0.01)	0.12 (0.06)	*Emiliania huxleyi*	~6000
LC+DFB	239 (8)	10.38 (1.31)	7.79 (0.35)	0.10 (0.08)	0.08 (0.08)	0.46 (0.03)	0.13 (0.19)	*Emiliania huxleyi*	~40000
HC+DFB	879 (16)	11.81 (0.30)	7.72 (0.14)	0.04 (0.06)	0.08 (0.06)	0.38 (0.07)	0.65 (0.07)	*Emiliania huxleyi*	~2000
HC-DFB	804 (29)	10.18 (1.15)	8.04 (0.09)	0.13 (0.07)	0.05 (0.06)	0.30 (0.09)	0.76 (0.33)	Small nanoeukaryotes	< 1000
d21									
LC-DFB	216 (32)	5.61 (0.20)	7.27 (0.11)	0.03 (0.05)	0.10 (0.02)	0.48 (0.02)	0.16 (0.11)	*Emiliania huxleyi*	~15000
LC+DFB	268 (24)	10.9 (1.25)	7.44 (0.13)	0.03 (0.05)	0.04 (0.03)	0.58 (0.06)	0.39 (0.24)	*Emiliania huxleyi*	~60000
HC+DFB	768 (49)	9.79 (1.69)	7.61 (0.40)	0.02 (0.05)	0.03 (0.04)	0.50 (0.08)	0.12 (0.10)	*Emiliania huxleyi*	~7000
HC-DFB	708 (38)	6.02 (0.69)	7.04 (0.34)	0.07 (0.00)	0.04 (0.04)	0.31 (0.01)	0.10 (0.09)	Small nanoeukaryotes	~3000

Biogeosciences Discuss., https://doi.org/10.5194/bg-2018-448
Manuscript under review for journal Biogeosciences
Discussion started: 19 November 2018

Table 3. The concentration of particulate metals in seawater (nmol L^{-1}) in the different treatments; LC: ambient CO_2 (390 µatm); HC: increased CO_2 (900 µatm); -DFB (ambient dFe); +DFB (increased dFe) during the development of a bloom of *Emiliania huxleyi*. Data are averages of replicate mesocoms and standard deviations are shown in brackets.

	Treatment	Al	Ti	P	Fe	Cu	Co (·10)	Zn	Cd (·100)	Mn	Mo	Pb (·10)
d12												
	LC-DFB	9.16 (3.16)	1.30 (0.27)	131.8 (27.05)	13.5 (0.88)	0.24 (0.04)	0.10 (0.06)	3.24 (0.15)	0.28 (0.06)	0.24 (0.06)	0.08 (0.01)	0.25 (0.01)
	LC+DFB	29.2 (6.00)	3.16 (0.52)	329.3 (107.8)	14.8 (1.78)	0.30 (0.01)	0.22 (0.05)	14.81 (2.69)	0.91 (0.22)	0.54 (0.14)	0.09 (0.02)	0.56 (0.05)
	HC+DFB	11.0 (7.04)	1.23 (0.54)	120.1 (45.49)	7.29 (0.41)	0.32 (0.09)	0.07 (0.01)	3.13 (0.55)	0.26 (0.23)	0.17 (0.06)	0.04 (0.02)	0.12 (0.05)
	HC-DFB	18.1 (8.53)	1.28 (0.53)	193.7 (66.43)	11.2 (4.43)	0.29 (0.08)	0.11 (0.07)	4.48 (0.38)	0.23 (0.03)	0.29 (0.13)	0.07 (0.01)	0.85 (0.51)
d17												
	LC-DFB	27.1 (14.8)	0.27 (0.14)	171.6 (20.1)	17.1 (8.08)	0.10 (0.04)	0.07 (0.00)	2.87 (1.23)	0.45 (0.32)	0.20 (0.04)	0.08 (0.05)	0.28 (0.11)
	LC+DFB	29.2 (19.2)	4.63 (2.84)	972.8 (563)	12.2 (9.14)	1.02 (0.56)	0.68 (0.42)	62.7 (38.2)	2.38 (0.87)	2.36 (1.49)	0.37 (0.08)	0.77 (0.41)
	HC+DFB	5.94 (4.38)	0.59 (0.34)	134.1 (47.7)	1.98 (0.76)	0.13 (0.07)	0.05 (0.02)	2.53 (0.49)	0.19 (0.03)	0.14 (0.04)	0.06 (0.03)	0.14 (0.05)
	HC-DFB	35.4 (17.9)	4.11 (1.86)	372.7 (253)	9.34 (7.29)	0.50 (0.06)	0.19 (0.02)	5.88 (3.78)	0.98 (0.65)	0.56 (0.42)	0.09 (0.06)	1.42 (0.37)
d21												
	LC-DFB	19.2 (1.01)	2.95 (0.06)	341.9 (20.1)	5.83 (1.81)	0.48 (0.02)	0.35 (0.03)	15.5 (0.97)	1.13 (0.26)	0.66 (0.06)	0.10 (0.02)	2.07 (0.26)
	LC+DFB	9.18 (5.35)	1.53 (0.55)	380.9 (45.3)	2.52 (0.35)	0.44 (0.06)	0.37 (0.07)	26.2 (2.96)	1.41 (0.25)	0.88 (0.09)	0.20 (0.05)	1.23 (0.75)
	HC+DFB	2.64 (1.58)	0.49 (0.40)	95.9 (12.5)	0.53 (0.32)	0.15 (0.06)	0.09 (0.04)	3.24 (1.96)	0.30 (0.16)	0.14 (0.05)	0.05 (0.01)	0.19 (0.05)
	HC-DFB	8.22 (2.05)	0.87 (0.20)	134.7 (22.1)	3.19 (1.21)	0.26 (0.05)	0.12 (0.02)	3.47 (0.97)	0.27 (0.13)	0.22 (0.08)	0.08 (0.03)	0.58 (0.18)

Biogeosciences Discuss., https://doi.org/10.5194/bg-2018-448
Manuscript under review for journal Biogeosciences
Discussion started: 19 November 2018

Table 4. The concentration of particulate metals in seawater (nmol L^{-1}) in the different treatments after oxalate-wash; LC: ambient CO_2 (390 µatm); HC: increased CO_2 (900 µatm); -DFB (ambient dFe); +DFB (increased dFe) during the development of a bloom of *Emiliania huxleyi*. Data are averages of replicate mesocoms and standard deviations are shown in brackets. The percentage (%) indicates the mean quantity of metal remaining after the oxalate wash. Statistically significant differences are indicated with asterisk (* if p <0.05; ** if p <0.01 and *** if p<0.001; ns: not significant).

	Treatment	Al	Ti	P	Fe	Cu	Co (·10)	Zn	Cd (·100)	Mn	Mo	Pb (·10)
d12												
	LC-DFB	11.6 (2.8)	1.32 (0.34)	117 (3.27)	12.52 (0.78)	0.16 (0.03)	0.07 (0.00)	1.92 (0.86)	0.09 (0.06)	0.15 (0.02)	0.02 (0.00)	0.10 (0.00)
	LC+DFB	28.3 (12)	4.49 (1.91)	258 (46.1)	14.67 (3.35)	0.23 (0.08)	0.19 (0.00)	7.16 (1.29)	0.51 (0.14)	0.41 (0.06)	0.03 (0.01)	0.20 (0.11)
	HC+DFB	15.9 (2.3)	2.52 (0.66)	139 (14.2)	8.05 (1.08)	0.22 (0.06)	0.09 (0.01)	2.39 (0.93)	0.20 (0.09)	0.21 (0.07)	0.03 (0.01)	0.11 (0.06)
	HC-DFB	11.6 (8.8)	1.66 (0.68)	178 (66.3)	9.79 (3.75)	0.19 (0.08)	0.08 (0.03)	2.84 (0.52)	0.22 (0.06)	0.28 (0.08)	0.02 (0.01)	0.19 (0.08)
d17												
	LC-DFB	6.42 (2.9)	0.85 (0.35)	97 (41.6)	1.23 (0.56)	0.11 (0.07)	0.09 (0.05)	2.86 (1.45)	0.26 (0.09)	0.18 (0.07)	0.03 (0.00)	0.09 (0.05)
	LC+DFB	7.53 (4.7)	1.85 (0.63)	245 (136)	1.28 (0.68)	0.24 (0.11)	0.22 (0.08)	12.1 (3.78)	1.20 (0.69)	0.54 (0.29)	0.05 (0.03)	0.18 (0.09)
	HC+DFB	4.48 (0.2)	1.29 (0.01)	131 (5.31)	1.55 (0.19)	0.14 (0.01)	0.07 (0.00)	3.03 (0.90)	0.21 (0.06)	0.14 (0.02)	0.03 (0.00)	0.10 (0.05)
	HC-DFB	12.8 (2.7)	1.98 (0.74)	233 (162)	5.31 (0.99)	0.29 (0.11)	0.18 (0.06)	5.03 (3.06)	0.35 (0.13)	0.43 (0.33)	0.06 (0.01)	0.24 (0.02)
d21												
	LC-DFB	13.9 (3.2)	1.54 (0.48)	257 (20.9)	3.76 (0.75)	0.29 (0.06)	0.26 (0.01)	8.59 (0.69)	0.74 (0.31)	0.35 (0.04)	0.05 (0.02)	0.21 (0.08)
	LC+DFB	4.36 (0.4)	1.01 (0.41)	253 (47.6)	2.04 (0.63)	0.23 (0.02)	0.20 (0.01)	14.3 (1.32)	0.67 (0.09)	0.43 (0.05)	0.05 (0.01)	0.09 (0.02)
	HC+DFB	2.49 (0.9)	0.62 (0.17)	79 (19.6)	0.33 (0.07)	0.11 (0.02)	0.07 (0.03)	2.36 (1.38)	0.09 (0.06)	0.09 (0.03)	0.01 (0.00)	0.03 (0.01)
	HC-DFB	2.56 (1.2)	0.98 (0.30)	74 (20.7)	1.03 (0.18)	0.12 (0.03)	0.05 (0.01)	1.01 (0.35)	0.05 (0.02)	0.07 (0.01)	0.02 (0.00)	0.13 (0.01)
	%	ns	ns	80*	75*	60*	70*	55**	45***	55**	35***	30***

*ns: not significant; * p <0.05; ** p <0.01; *** p<0.001*

Biogeosciences Discuss., https://doi.org/10.5194/bg-2018-448
Manuscript under review for journal Biogeosciences
Discussion started: 19 November 2018

Table 5. Statistical analyses (Split-plot ANOVA) of the effects of CO_2, DFB, and their interaction, as well as the effect of time, on the concentrations of particulate metals in seawater (A) and on the oxalate-washed concentrations of particulate metals in seawater (B) in the different treatments LC: ambient CO_2 (390 µatm); HC: increased CO_2 (900 µatm); -DFB (ambient dFe); +DFB (increased dFe) during the development of a bloom of *Emiliania huxleyi*. Statistically significant differences are indicated with asterisk (* if p <0.05; ** if p <0.01, and *** if p<0.001; ns: not significant).

(A)

Factor	Al	Ti	P	Fe	Cu	Co	Zn	Cd	Mn	Mo	Pb
Carbon	ns	ns	**	*	ns	**	***	***	**	***	ns
DFB	ns	ns	*	ns	ns	*	**	ns	*	*	ns
Carbon x DFB	ns	*	**	ns	ns	*	**	*	**	**	ns
Time	ns	ns	ns	***	*	***	***	***	***	***	**

(B)

Factor	Al	Ti	P	Fe	Cu	Co	Zn	Cd	Mn	Mo	Pb
Carbon	ns	ns	ns	ns	ns	***	***	***	*	*	ns
DFB	ns	*	ns	ns	ns	ns	*	ns	ns	ns	ns
Carbon x DFB	ns	ns	*	ns	*	ns	*	*	**	*	ns
Time	**	***	**	***	ns	*	*	*	ns	**	*

*ns: not significant; * p <0.05; ** p <0.01; *** p<0.001*

Biogeosciences Discuss., https://doi.org/10.5194/bg-2018-448
Manuscript under review for journal Biogeosciences
Discussion started: 19 November 2018

Table 6. The relationship (Pearson correlations, $p < 0.05$) between particulate metals concentrations (nmol L^{-1}) and the biomass (µgC L^{-1}) of *Emiliania huxleyi* and total cells (phytoplankton and microzooplankton) obtained from Segovia et al. (2017) during the bloom.

		P	Fe	Cu	Co	Zn	Cd	Mn	Mo	Pb	Ti
(A) Samples without treatment											
E. huxleyi	Correlation coefficient	0.622	ns	0.614	0.756	0.747	0.818	0.686	0.825	ns	ns
	P-value	0.003		0.003	$7.35 \cdot 10^{-5}$	$1.01 \cdot 10^{-4}$	$6.02 \cdot 10^{-6}$	$5.93 \cdot 10^{-4}$	$4.20 \cdot 10^{-6}$		
Total cells	Correlation coefficient	0.641	ns	0.51	0.644	0.889	0.802	0.598	0.53	ns	ns
	P-value	0.002		0.02	$1.62 \cdot 10^{-3}$	$7.03 \cdot 10^{-8}$	$1.23 \cdot 10^{-5}$	$4.18 \cdot 10^{-3}$	$1.35 \cdot 10^{-2}$		
(B) Oxalate-washed samples											
E. huxleyi	Correlation coefficient	0.647	ns	0.637	0.770	0.758	0.826	0.702	0.819	ns	ns
	P-value	0.002		0.002	$4.52 \cdot 10^{-5}$	$6.79 \cdot 10^{-5}$	$3.92 \cdot 10^{-6}$	$3.86 \cdot 10^{-4}$	$5.68 \cdot 10^{-6}$		
Total cells	Correlation coefficient	0.513	ns	0.569	0.656	0.886	0.809	0.605	0.513	ns	ns
	P-value	0.02		0.009	$1.25 \cdot 10^{-3}$	$9.53 \cdot 10^{-8}$	$8.98 \cdot 10^{-6}$	$3.68 \cdot 10^{-3}$	0.0175		

Biogeosciences Discuss., https://doi.org/10.5194/bg-2018-448
Manuscript under review for journal Biogeosciences
Discussion started: 19 November 2018

Table 7. *P*-values for the effects of CO_2, DFB, their interaction and time on the P-normalized metal quotes (A) and on the oxalate-washed concentrations of P-normalized metal quotes (B) during the development of the bloom of *Emiliania huxleyi*. Statistically significant differences are indicated with asterisk (* if $p < 0.05$; ** if $p < 0.01$ and *** if $p < 0.001$).

A)

Factor	Fe:P	Cu:P	Co:P	Zn:P	Cd:P	Mn:P	Mo:P	Pb:P	Ti:P
Carbon	ns	*	***	**	ns	*	ns	ns	ns
DFB	ns	ns	ns	ns	ns	ns	ns	ns	ns
Carbon x DFB	ns	ns	ns	ns	ns	ns	ns	ns	ns
Time	***	***	***	***	ns	ns	ns	ns	***

B)

Factor	Fe:P	Cu:P	Co:P	Zn:P	Cd:P	Mn:P	Mo:P	Pb:P	Ti:P
Carbon	ns	**	***	**	***	**	ns	ns	ns
DFB	*	*	**	ns	**	**	ns	ns	ns
Carbon x DFB	ns	ns	ns	ns	*	**	ns	ns	ns
Time	***	*	***	***	***	ns	***	ns	**

*ns: not significant; * $p < 0.05$; ** $p < 0.01$; *** $p < 0.001$*

Biogeosciences Discuss., https://doi.org/10.5194/bg-2018-448
Manuscript under review for journal Biogeosciences
Discussion started: 19 November 2018

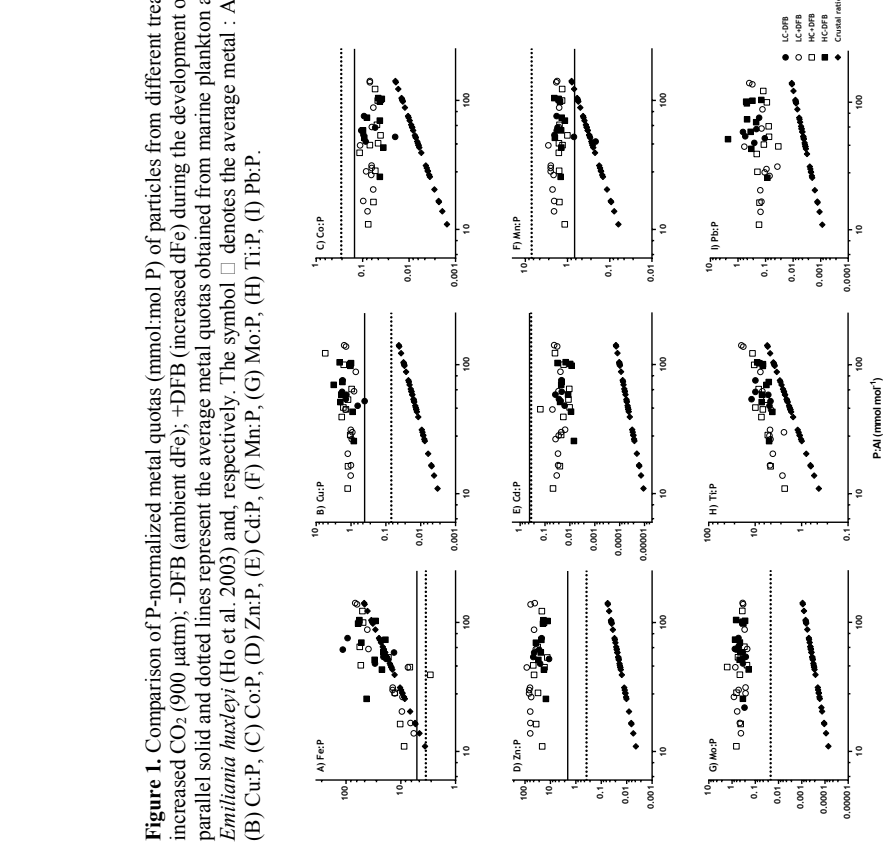

Figure 1. Comparison of P-normalized metal quotas (mmol:mol P) of particles from different treatments; LC: ambient CO_2 (390 µatm); HC: increased CO_2 (900 µatm); -DFB (ambient dFe); +DFB (increased dFe) during the development of a bloom of *Emiliania huxleyi*. The x-axis parallel solid and dotted lines represent the average metal quotas obtained from marine plankton assemblages (Ho 2006) and from cultures of *Emiliania huxleyi* (Ho et al. 2003) and, respectively. The symbol □ denotes the average metal : Al in crustal material (Taylor, 1964). (A) Fe:P, (B) Cu:P, (C) Co:P, (D) Zn:P, (E) Cd:P, (F) Mn:P, (G) Mo:P, (H) Ti:P, (I) Pb:P.